Electronic Supplementary Material (ESI) for Materials Chemistry Frontiers.

Flexible Control of Excited State Transition under Pressure/Temperature: Distinct Stimuli-Responsive Behaviours of Two ESIPT Polymorphs

Aisen Li,[a,b] Hao Liu,[a] Chongping Song,[a] Yijia Geng,[a] Shuping Xu,[a] Hongyu Zhang,[a] Houyu Zhang,[a] Haining Cui,[b] and Weiqing Xu[a]*

[a] State Key Laboratory of Supramolecular Structure and Materials, College of Chemistry, Jilin University, Changchun, P. R. China 130012
[b] College of Physics, Jilin University, Changchun, P. R. China 130012

*Email: xuwq@jlu.edu.cn

Contents

1. Stacking Structure

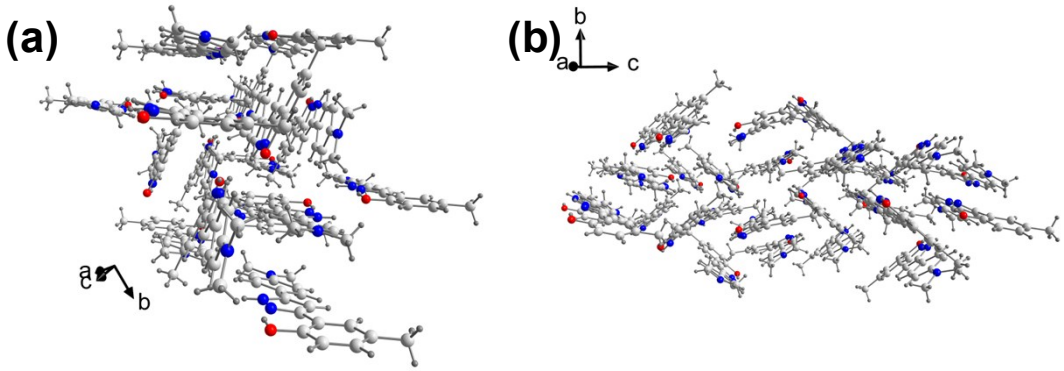

Figure S1. The stacking modes of GC (a) and BVC cells (b), respectively.

2. Summary of Intramolecular and Intermolecular Interactions

Table S1: The analysis of bond distances and bond angles of GC and BVC.

		GC	BVC	
			Nearly planar	Twisted
Distance (Å)		1.7069	1.7995	1.8809
Angle (deg)	C-O-H	104.333	108.137	109.460
	O-H…N	151.504	146.345	146.323
	H…N-C	100.077	97.213	99.59
Twisted Angle	C-C-C-N	5.575	5.345	20.708

Table S2.The analysis of bond distances and bond angles between two 4MPP in BVC.

Orientation of interaction	Distance (Å)	Angle (deg)
CH/N Me to N1	3.3966	132.036
CH/N Me to N1	3.4215	131.975
CH/N Me to N2	4.2441	125.325
CH/N Me to N2	4.1570	125.765
CH/N Ph2 to N1	3.7122	120.644
CH/N Ph2 to N2	3.8641	111.431
CH/O Me to O	3.3746	160.199

Table S3: The analysis of the bond distances and bond angles in GC.

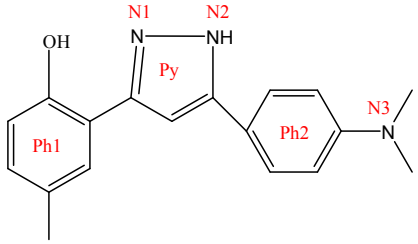

Orientation of interaction		Distance (Å)	Angle (deg)
NH/O	N2 to O	2.0934	143.544
OH/N	O to N1	2.9550	102.108
NH/π	N2 to Py	4.3651	112.750
CH/N	Py to N2	3.7765	104.817
CH/N	Ph2 to N2	3.5018	113.112
CH/N	Me to N1	3.0530	131.513
CH/N	Me to N2	3.0519	145.235
CH/π	Ph2 to Ph1	3.2109	141.655
CH/π	Me to Ph1	3.5966	140.875
CH/π	Me to Py	3.7218	108.255
CH/π	Me to Py	3.0918	120.843
CH/π	Ph2 to Py	2.8543	147.733
CH/π	Py to Ph1	3.7655	159.341
π/π	Ph2 to Ph2	3.7740	
CH/O	Ph2 to O	2.9253	161.970
CH/O	Ph2 to O	3.0791	113.758
CH/O	Me to O	3.0506	154.549

Table S4: The analysis of the bond distances and bond angles in BVC.

Orientation of interaction		Distance (Å)	Angle (deg)
π/π	Ph2 to Ph2	3.9428	
CH/N	Me to N1	4.1150	119.694
CH/N	Me to N2	3.4219	122.502
CH/N	Me to N2	3.5531	108.611
CH/N	Ph to N2	2.8571	162.151
CH/N	Ph to N1	2.9774	135.764
CH/N	Ph to N1	3.5353	123.882
CH/O	Me to O	3.6420	118.421
CH/O	Me to O	3.0567	141.070
CH/O	Me to O	3.3746	160.199
CH/O	Me to O	3.1592	102.780
CH/O	Me to O	4.1063	151.464
CH/O	Ph1 to O	2.9591	122.454
CH/O	Ph1 to O	4.1020	141.226
CH/O	Ph2 to O	2.7753	168.682
CH/O	Ph2 to O	3.0549	160.199
CH/O	Py to O	2.3315	112.896

3. Absorption Spectra of GC and BVC

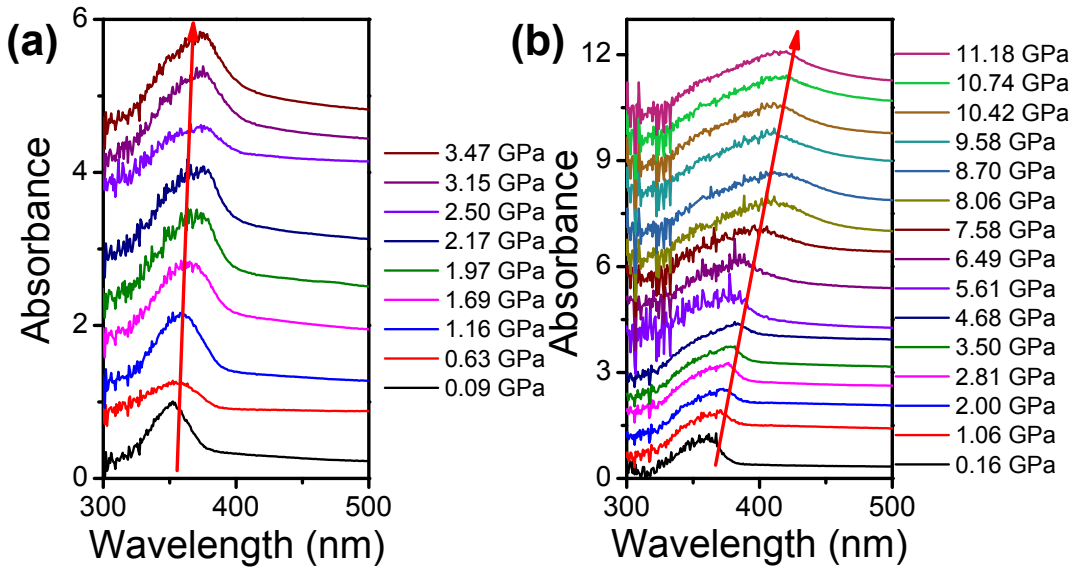

Figure S2. UV−visible absorption spectra of GC (a) and BVC (b) with increasing pressure.

4. Fluorescence Spectra of BVC.

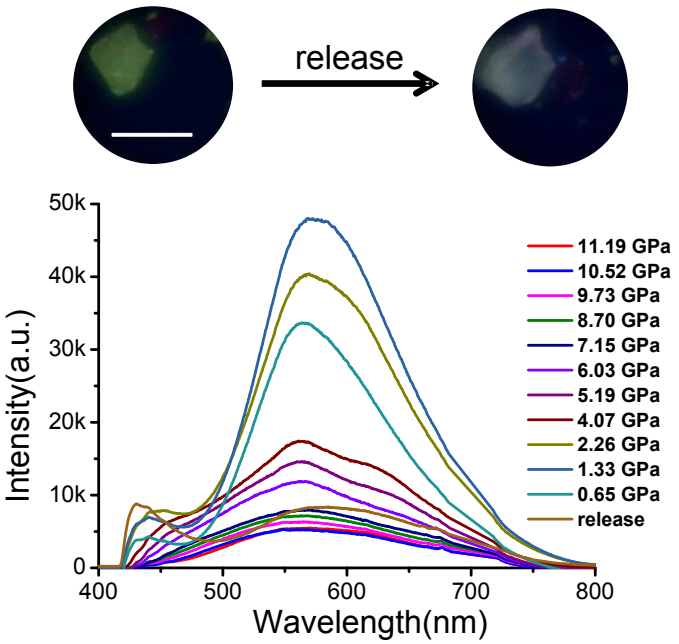

Figure S3. Fluorescent spectra of BVC at different pressure values *via* DAC (a) and the corresponding fluorescent photos (b) during the depressurizing process. Excitation wavelength was 365 nm. The scale is 100 μm.

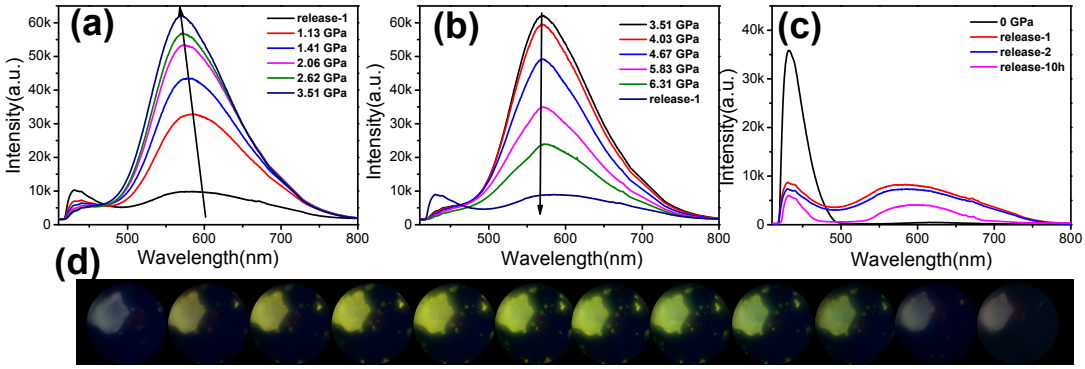

Figure S4. Fluorescent spectra of BVC crystal under the pressure from 0 to 3.61 GPa (a), from 3.61 to 6.31 GPa (b) and recovery (c). (d) Left to right; the photos during the compression under the excitation of 365 nm.

5. Raman Spectra under Hydrostatic Pressure

Table S5. Assignments and frequencies (cm^{-1}) of the observed Raman modes of GC and BVC, in comparison with DFT calculation results.

GC (cm^{-1})	BVC (cm^{-1})	Theoretical value (cm^{-1})	vibrational mode
160	160	163	methyl wagging vibration out of plane
198	196	193	C-C stretching vibration
355	355	361	methyl wagging vibration in plane
397	399	386	N-H and C-N wagging vibration out of plane
-	477	461	N-H and C-N wagging vibration out of plane
491	491	489	N-H and C-H wagging vibration out of plane, C-N wagging vibration in plane
686	684	684	O-H wagging vibration out of plane
710	709	708	C-H wagging vibration out of plane(Py and Ph1)
760	759	775	C-N stretching vibration, ring breathing vibration (Ph1)
870	867	888	ring breathing vibration (Ph1)
951	945	955	C-H wagging vibration out of plane
960	957	968	ring breathing vibration (Ph2), C-N stretching vibration
-	7732	1146	methyl wagging vibration out of plane
1170	1167	1161	C-H wagging vibration in plane(Ph2)
1181	1193	1219	C-H wagging vibration in plane
1190	1205	1233	C-H wagging vibration in plane
1254	1244	1247	C-H and O-H wagging vibration in plane
1264	1260	1276	ring breathing vibration (Ph2),C-H wagging vibration in plane
1285	1284	1291	N=N stretching vibration, C-H and O-H wagging vibration in plane
1370	1368	1372	ring breathing vibration (Ph2)
1399	1398	1413	N-H,O-H and C-H wagging vibration in plane, C=C stretching vibration
1446	1441	1443	N-H,O-H and C-H wagging vibration in plane
1477	1471	1485	ring breathing vibration, O-H wagging vibration in plane

1514	1512	1510	N-H and O-H wagging vibration in plane, C-C stretching vibration
1616	1613	1623	C-C and C=C stretching vibration, O-H and N-H wagging vibration in plane
1626	1627	1675	C-C and C=C stretching vibration
2799	2860	3002	methyl symmetrical stretching vibration (N-CH_3)
2909	2905	3030	methyl symmetrical stretching vibration (Ph1)
2966	2966	3065	methyl antisymmetric stretching vibration
3381	3379	-	O-H stretching vibration
-	3421	-	N-H stretching vibration

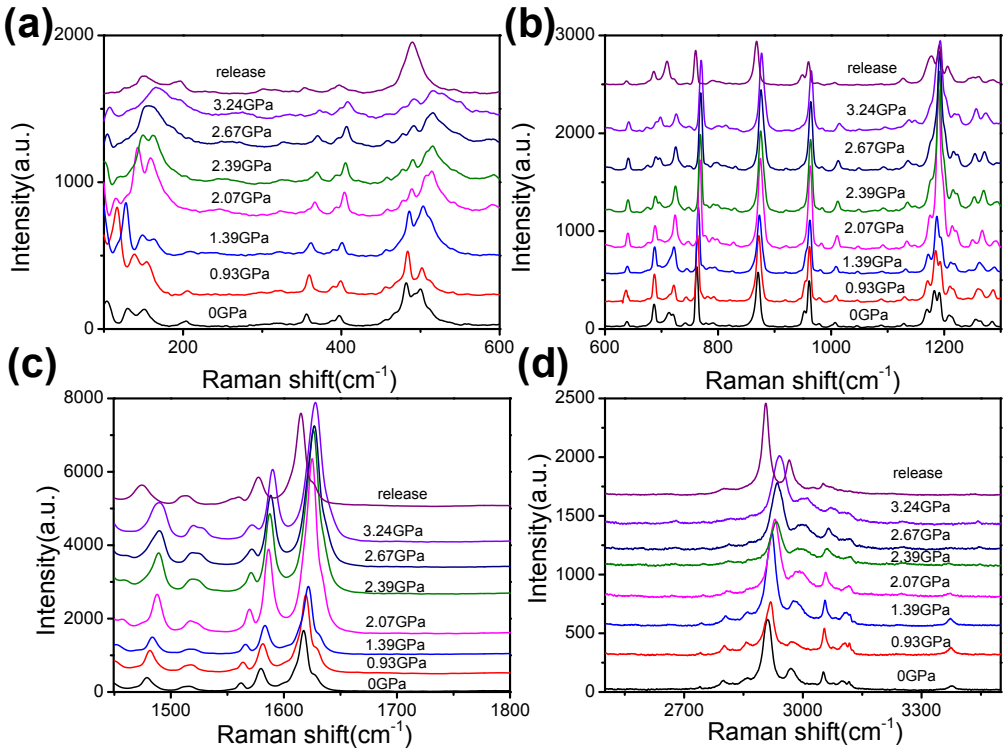

Figure S5. Raman spectra of GC at different pressure values *via* DAC. The excitation wavelength was 633 nm. (a)-(d) 100-600, 600-1320, 1400-1800, and 2400-3500 cm^{-1}, respectively.

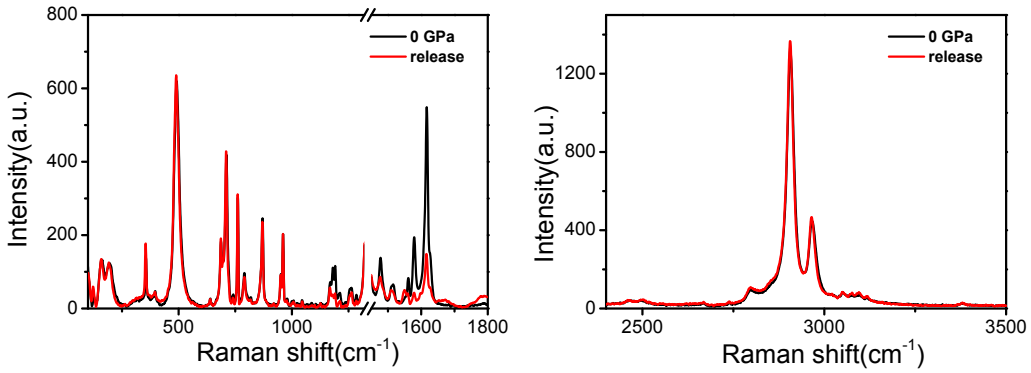

Figure S6. The recovery of the Raman spectra of GC under the excitation of 633 nm. Left panel; 100-1800 cm^{-1}. Right panel: 2400-3500 cm^{-1}.

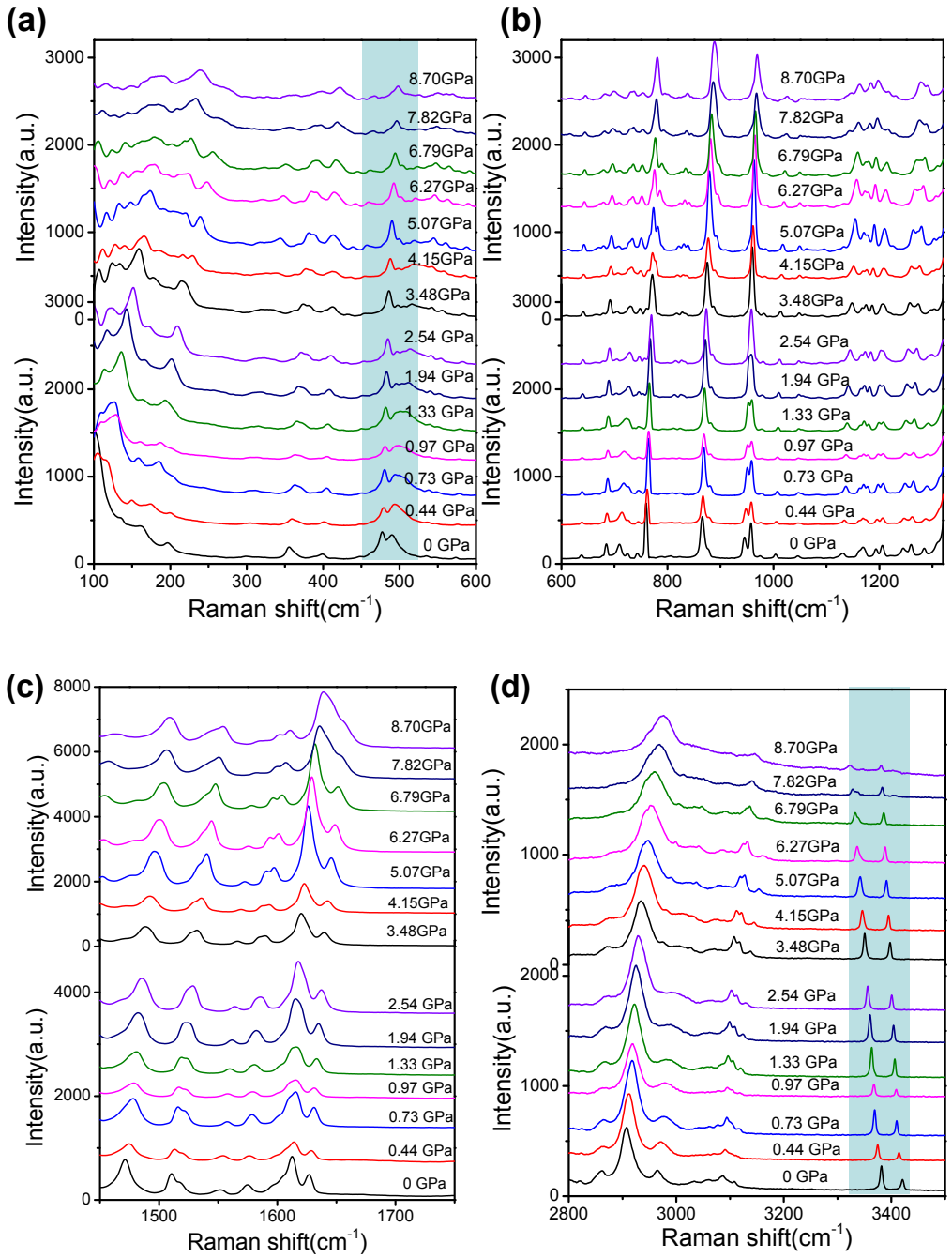

Figure S7. Raman spectra of BVC at different pressure values *via* DAC. Excitation wavelength was 633 nm. (a)-(d) 100-600, 600-1320, 1400-1800, and 2400-3500 cm^{-1}, respectively.

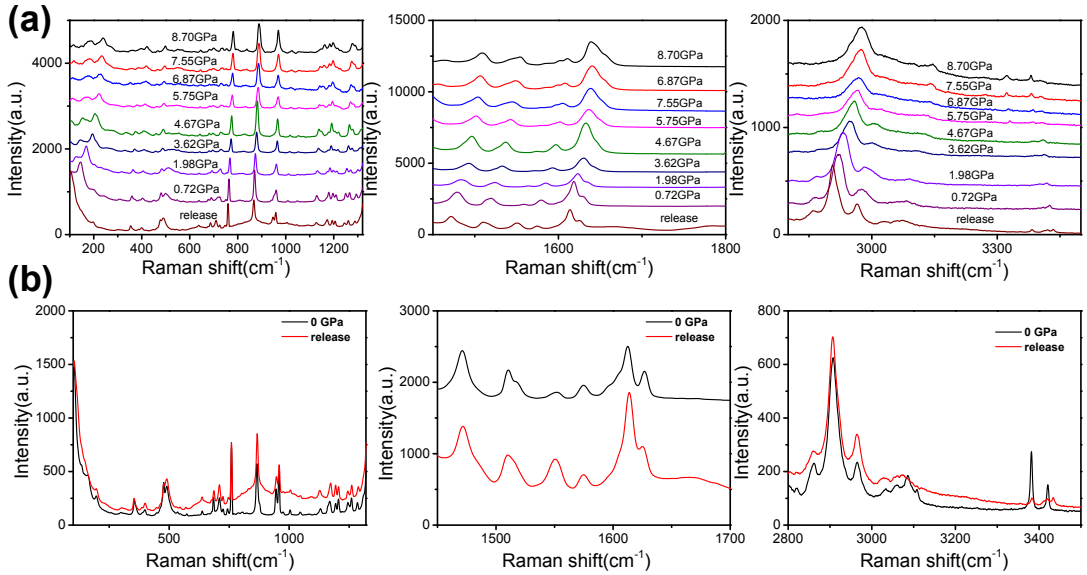

Figure S8. Raman spectra of BVC during the decompression (a) and the recovery properties (b). Excitation wavelength was 633 nm.

6. The Analysis of Theoretical Results

Table S6. Optimized lattice parameters of BVC under different external pressures.

Stress	a/Å	b/Å	c/Å	α/°	β/°	γ/°	V/Å^3
Exp. Data	16.236(3)	7.7124(15)	25.238(5)	90	104.08(3)	90	3065.40
0 GPa	16.6290	8.6641	27.6758	90	102.4970	90	3892.90
1.0 GPa	16.1727	8.1122	24.6041	90	103.9450	90	3132.84
2.0 GPa	16.0589	7.5993	24.3802	90	104.6144	90	2879.03
3.0 GPa	15.8201	7.4041	24.0972	90	105.2938	90	2722.64
4.0 GPa	15.7852	7.1938	23.9992	90	105.4720	90	2626.50
5.0 GPa	15.5499	7.0939	23.8046	90	105.7533	90	2527.27
6.0 GPa	15.5172	6.9715	23.7303	90	105.8446	90	2469.58
7.0 GPa	15.4652	6.8961	23.4867	90	105.9813	90	2408.03
8.0 GPa	15.4316	6.8050	23.4223	90	106.0749	90	2363.44

Table S7. The distances of the intramolecular hydrogen bond (O-H…N) in a 4MPP molecule based on a twisted conformation in BVC in optimized unit cell under different external pressures.

Stress \ Distance (Å)	O-H	H…N	O…N	Angle/º
Exp. Data	0.971	1.799	2.663	146.34
0 GPa	0.999	1.715	2.618	148.39
1.0 GPa	1.001	1.699	2.606	149.59
2.0 GPa	1.002	1.685	2.595	148.99
3.0 GPa	1.002	1.685	2.597	149.12
4.0 GPa	1.004	1.668	2.584	149.56
5.0 GPa	1.004	1.678	2.591	14921
6.0 GPa	1.005	1.663	2.580	149.50
7.0 GPa	1.006	1.658	2.576	149.58
8.0 GPa	1.007	1.648	2.568	149.69

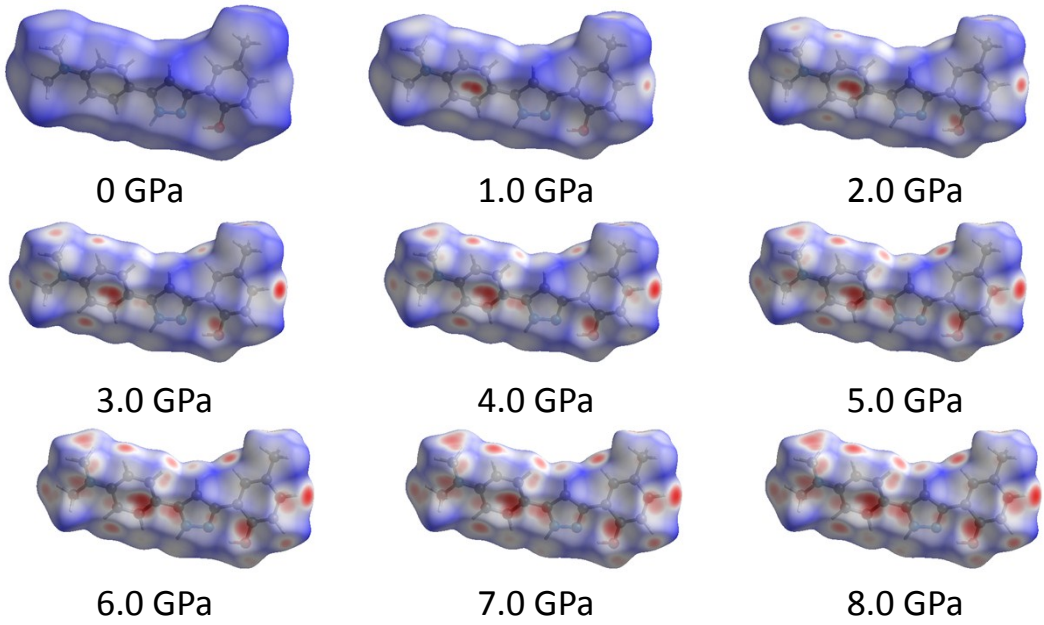

Figure S9. Hirshfeld surfaces of a 4MPP molecule based on a twisted conformation in BVC under different pressures.

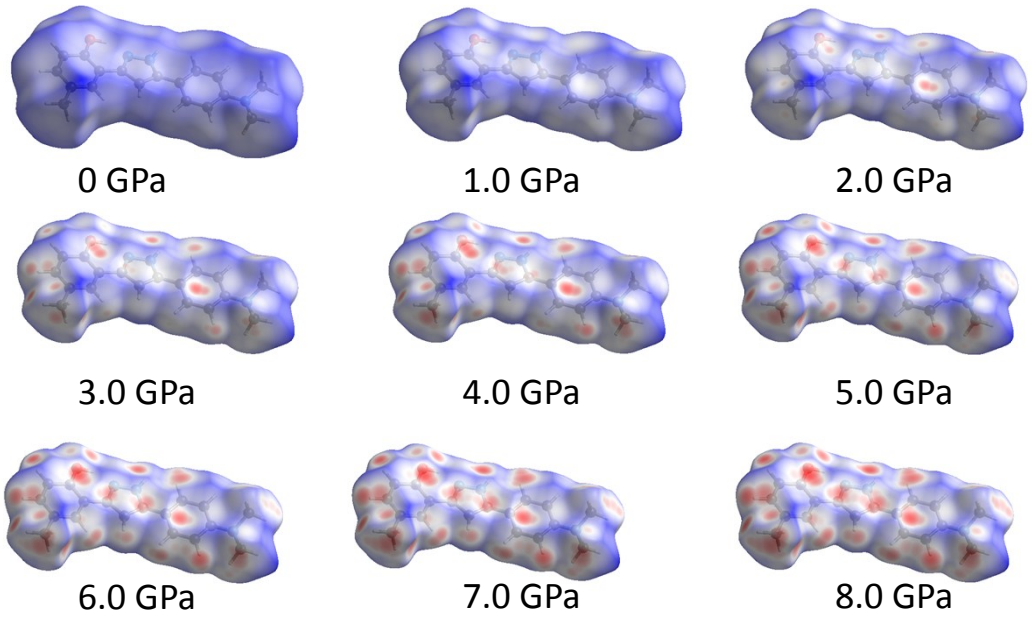

Figure S10. Hirshfeld surfaces of a 4MPP molecule based on nearly planar conformation in BVC under different pressures.

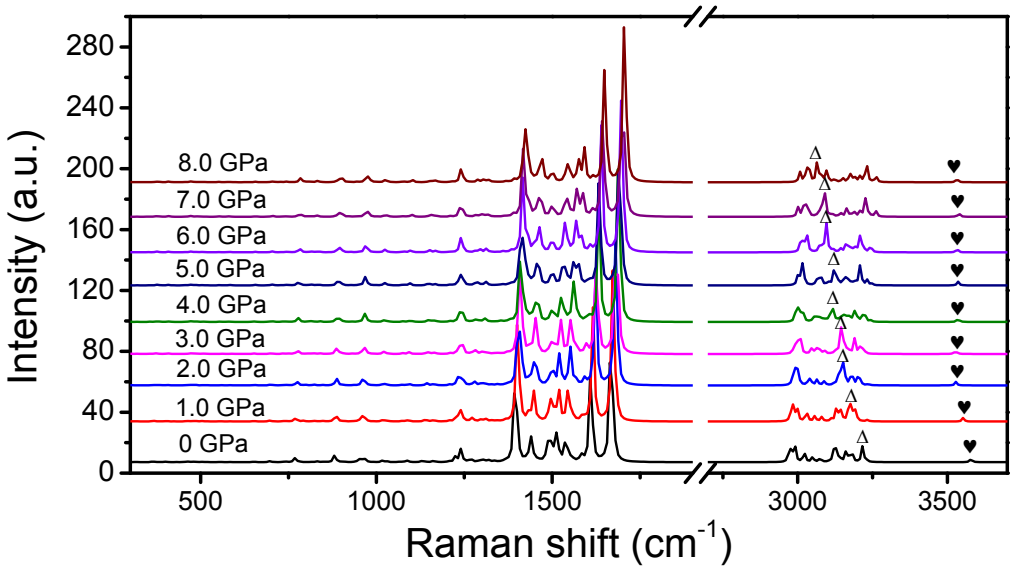

Figure S11. The calculated Raman spectra of a 4MPP molecule based on a twisted conformation in BVC under the external stress of 0, 1.0, 2.0, 3.0, 4.0, 5.0, 6.0, 7.0 and 8.0 Gpa. The symbol "Δ" and "♥" represents the O-H and the N-H stretching vibrational modes, respectively.

7. Temperature-Dependent Fluorescent Photos and Spectra

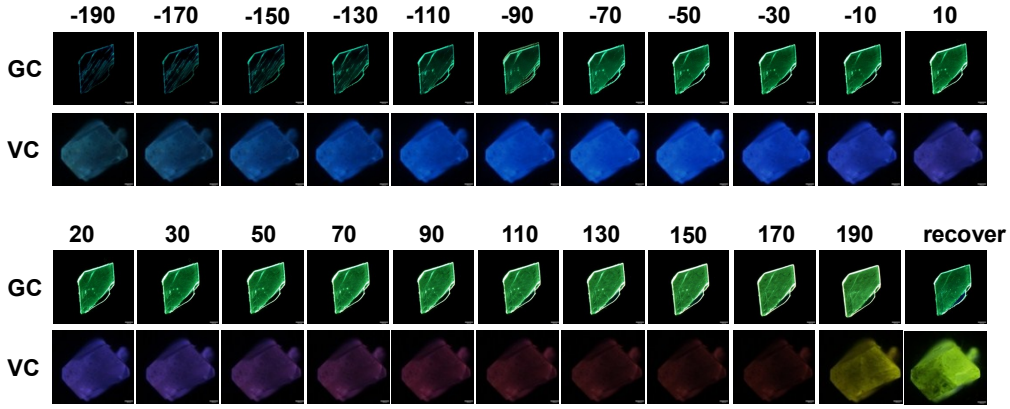

Figure S12. Temperature-dependent fluorescent photos of GC and BVC during -190℃-190 ℃. λex =375 nm.

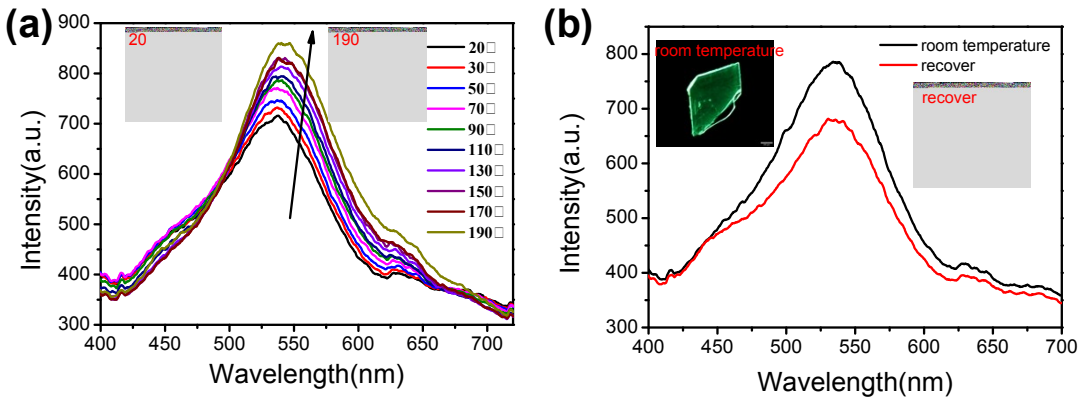

Figure S13. Temperature-dependent fluorescent spectra of GC during 20 ℃-190 ℃ (a) and reversible fluorescence switching with temperature (b). λex =375 nm.

8. Recovery Feature

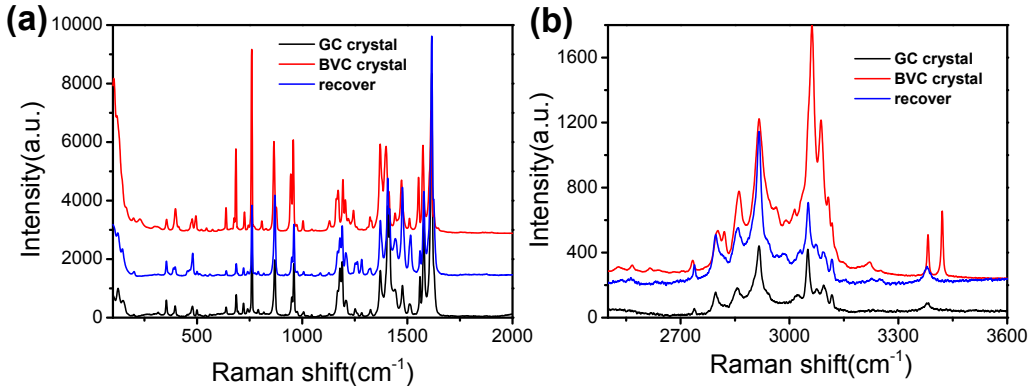

Figure S14. The comparison of Raman spectra of GC, BVC and the crystals recovered to the room temperature. Excitation wavelength was 633 nm.

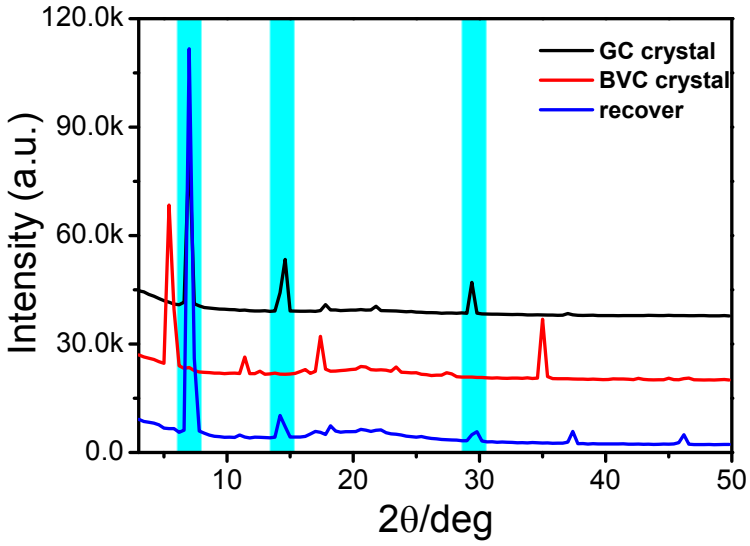

Figure S15. XRD patterns of GC, BVC and the crystal that recovers to room temperature.

Table S8. Data summary for the obtained single crystal of GC, BVC, and the recovered BVC from 190℃.

	GC	BVC	RECOVER
Sum formula	C18 H19 N3 O	C18 H19 N3 O	C18 H19 N3 O
Formula wt	293.36	293.36	293.36
T,K	296 K	293 K	276 K
Space group	P 1 21/c 1	P 1 21/n 1	P 1 21/c 1
Hall group	-P 2ybc	-P 2yn	-P 2ybc
A, Å	12.841(3)	16.236(3)	12.8182(18)
B, Å	10.286(2)	7.7124(15)	10.2860(15)
C, Å	12.663(3)	25.238(5)	12.6234(17)
α, deg	90	90	90
β, deg	111.023(7)	104.08(3)	110.977(5)
γ, deg	90	90	90
Volume, $Å^3$	1561.1(7)	3065.4(11)	1554.1(4)
Z	4	8	4
Density, Mg / m^3	1.248	1.271	1.254
$\mu(M_0 K \alpha)$, mm^{-1}	0.079	0.081	0.080
R(reflections)	0.0470(1958)	0.0509(3670)	0.0822(1661)
wR2(reflections)	0.1241(2771)	0.1550(6863)	0.3052(3581)
Goodness of fit	0.994	0.978	0.997
CCDC	1576929	1576917	